

NPS ARCHIVE
1962
WOOD, F.

TEMPER BRITTLENESS RELATED TO FAULTING

FRED L. WOOD

LIBRARY
U.S. NAVAL POSTGRADUATE SCHOOL
MONTEREY, CALIFORNIA

TEMPER BRITTLENESS RELATED TO FAULTING

* * * * *

Fred L. Wood

TEMPER BRITTLENESS RELATED TO FAULTING

by

Fred L. Wood

Lieutenant, United States Navy

Submitted in partial fulfillment of
the requirements for the degree of

MASTER OF SCIENCE

United States Naval Postgraduate School
Monterey, California

1 9 6 2

NPS ARCHIVES

1962

WOOD, E.

~~Thesis~~
W78

LIBRARY
U.S. NAVAL POSTGRADUATE SCHOOL
MONTEREY, CALIFORNIA

TEMPER BRITTLENESS RELATED TO FAULTING

by

Fred L. Wood

This work is accepted as fulfilling
the thesis requirements for the degree of

MASTER OF SCIENCE

from the

United States Naval Postgraduate School

ABSTRACT

Temper brittleness was induced in a 3140 steel specimen by means of an isothermal heat treatment in a salt bath. Changes in internal structure of ductile and embrittled specimens were studied using a high-precision X-ray diffractometer. The resulting peak shapes showed (1) a slightly better resolution of the alpha doublet by the brittle specimen, (2) a relative peak displacement between similar lines in the ductile and brittle specimens, and (3) an asymmetry in some of the peak shapes. Based on the observed asymmetry of some of the diffraction peak shapes and published results of other workers using the electron microscope, it is suggested that the embrittlement is related to stacking faults in the crystal structure. Comments are also offered as a possible explanation of the transition curve.

The writer wishes to express his appreciation for the assistance, many helpful suggestions, and the encouragement given him by Professor John R. Clark, of the U. S. Naval Postgraduate School, during this investigation. He also wishes to thank Mrs. Norma Stevens for doing such a fine job of typing from rough notes.

TABLE OF CONTENTS

Section	Title	Page
1.	Introduction	1
2.	Theory	6
	Faulting in Crystals	6
	Fracture and Dislocations	9
	Partial Dislocations and Faulting	11
	Measurement of Faulting by Fourier Analysis of X-ray Diffraction Peak Shapes	13
3.	Experimental Work	18
4.	Results	22
	Results of Other Workers Using the Electron Microscope	24
5.	Conclusions	27
	Bibliography	29

LIST OF ILLUSTRATIONS

Figure	Page
1.	3a
2.	3a
3. Face Centered Cubic Structure	6a
4. Faulting on the (111) planes of a FCC metal	6a
5. Projection of BCC Structure on a (110) and a (112) plane	8a
6. Impact Energy vs. Temperature	19a
7. (112) Peak Ductile Specimen	22a
8. (112) Peak Brittle Specimen	22b
9. (110) Peak Brittle Specimen	23a
10. (110) Peak Ductile Specimen	23b
11. (112) Peak Ductile Specimen Temperature -47°C	26a
12. (112) Peak Brittle Specimen Temperature -47°C	26b
13. (112) Peak Ductile Specimen Room Temperature	26c
14. (112) Peak Brittle Specimen Room Temperature	26d
15. (112) Peak Ductile Specimen Temperature 90°C	26e
16. (112) Peak Brittle Specimen Temperature 90°C	26f

1. Introduction

Carbon steel plate, when stressed in an ordinary tension test, normally fails in a ductile manner, that is failure is preceded by some plastic deformation. The same material, however, under other conditions, can fail in a brittle fashion with no plastic deformation. Many brittle, catastrophic failures of steel structures have occurred. However the baffling problem for engineers and metallurgists who encounter the phenomenon is the fact that steel plate taken from a structure which has failed in a completely brittle manner shows a high degree of strength and ductility when tested in an ordinary tension test. This phenomenon has been extensively investigated and results of these investigations are summarized in review articles by Holloman¹, Woodfine², Polushkin³, and Queneau⁴.

The terms "brittleness" and "embrittlement", which can have the same meaning, are used by some people to describe completely different happenings. True brittleness is generally thought of as being associated with a low resistance to shock and a shattering upon fracture. Glass and some minerals exhibit this property. Embrittlement, on the other hand, usually refers to a relative decrease in the ductility of the specimen being considered after certain heat treatments. The tensile properties remain essentially unchanged and the difference in ductility is detected only by means of an impact or slow bend test. In this discussion the terms "brittleness" or "embrittlement" will refer to the relative change in ductility.

Many types of embrittlement are well known. Some of these are associated with large grain size, strain hardening, residual stresses, impurities

in solution with the metal, contained gases, discontinuities of grain boundaries, and a precipitation of hard particles from a solid solution. This last effect generally covers such topics as temper brittleness, blue brittleness, and overaging. The present investigation deals only with the phenomenon of temper brittleness.

Elongation as measured in a tensile test gives an inadequate index of ductility. Impact tests are necessary to bring out brittleness associated with such factors as heat treatment involving fast or slow cooling through a temperature range down to room temperature. Further investigation reveals that brittle behavior depends on the temperature at which the test is conducted and indicates that heat treatment or alloying does not necessarily cause brittleness per se, but raises or lowers a "transition" temperature resulting in ductile or brittle failure at the particular test temperature.

Temper brittleness as defined in the 1961 Metals Handbook⁵ is "Brittleness that results when certain steels are held within, or are cooled slowly through, a certain range of temperature below the transformation range. The brittleness is revealed by notched-bar impact tests at or below room temperature." This means that we are considering a relative brittleness since this embrittled specimen is compared with another specimen of the same material which has been quenched and is not embrittled.

Another term that must be defined before one can discuss temper brittleness is "transition temperature", referred to above. Again, in accordance with the 1961 Metals Handbook⁵, transition temperature is "(1) an arbitrarily defined temperature within the temperature range in which metal fracture characteristics determined usually by notched tests are changing rapidly such as from primarily fibrous (shear) to primarily

crystalline (cleavage) fracture. Commonly used definitions are 'transition temperature for 50% cleavage fracture', '10-ft-lb transition temperature'; and 'transition temperature for half maximum energy'. (2) Sometimes also used to denote the arbitrarily defined temperature in a range in which the ductility changes rapidly with temperature." The transition range can readily be seen if charpy impact energy is plotted as a function of temperature as in figure 1. At temperatures below T_A the failure would be brittle and above T_B the failure would be ductile. The transition range refers to the region between T_A and T_B .

Temper brittleness is not really an embrittlement but refers to a change in the transition temperature as can be seen in figure 2. Curve A refers to a ductile specimen while curve B is for an embrittled specimen of the same material. It is evident that the transition range of the brittle material occurs at a higher temperature than that of the ductile material. If both ductile and brittle specimens were to be broken on an impact tester at a temperature corresponding to T_3 there would be no apparent difference in the energy required to break them. If they should be broken at T_1 , again there would be no difference between them and one might consider, initially, that they were the same. However, at intervening temperatures, such as a temperature corresponding to T_2 , a noticeable difference will be observed. This important feature was first reported in 1944 by Jolivet and Vidal⁶. A structure designed on the basis of impact properties determined at temperature T_3 would be inadequate for service at a temperature corresponding to T_1 . This is the phenomenon that has led to the catastrophic brittle failures.

Brittle fracture has been an important problem for the Navy, especially

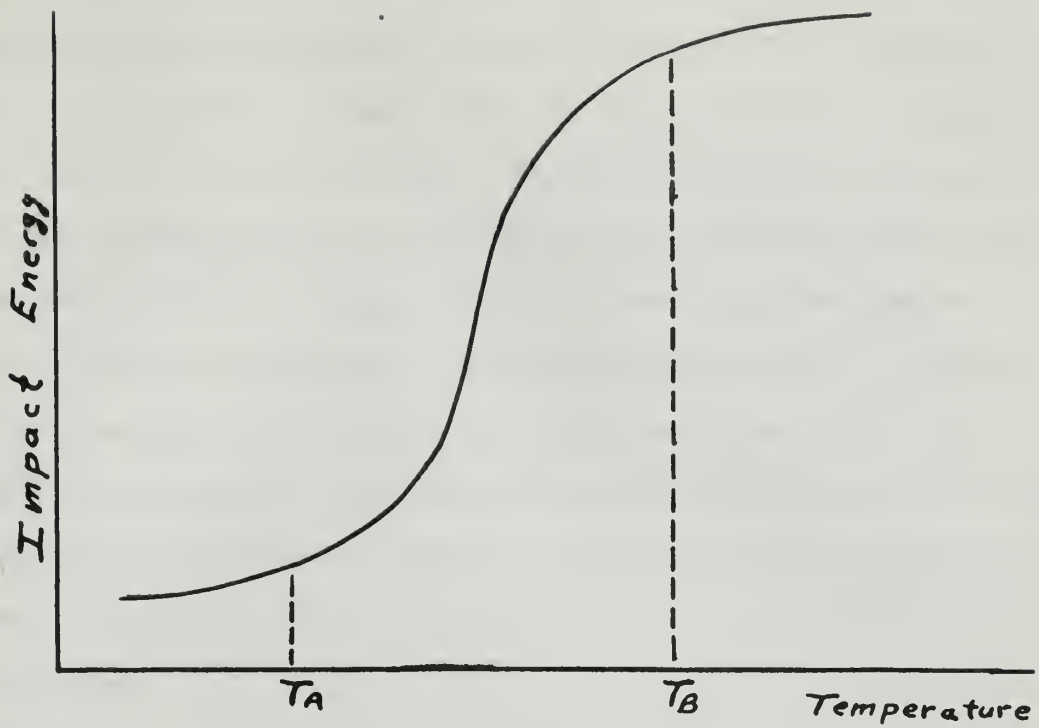


Figure 1.

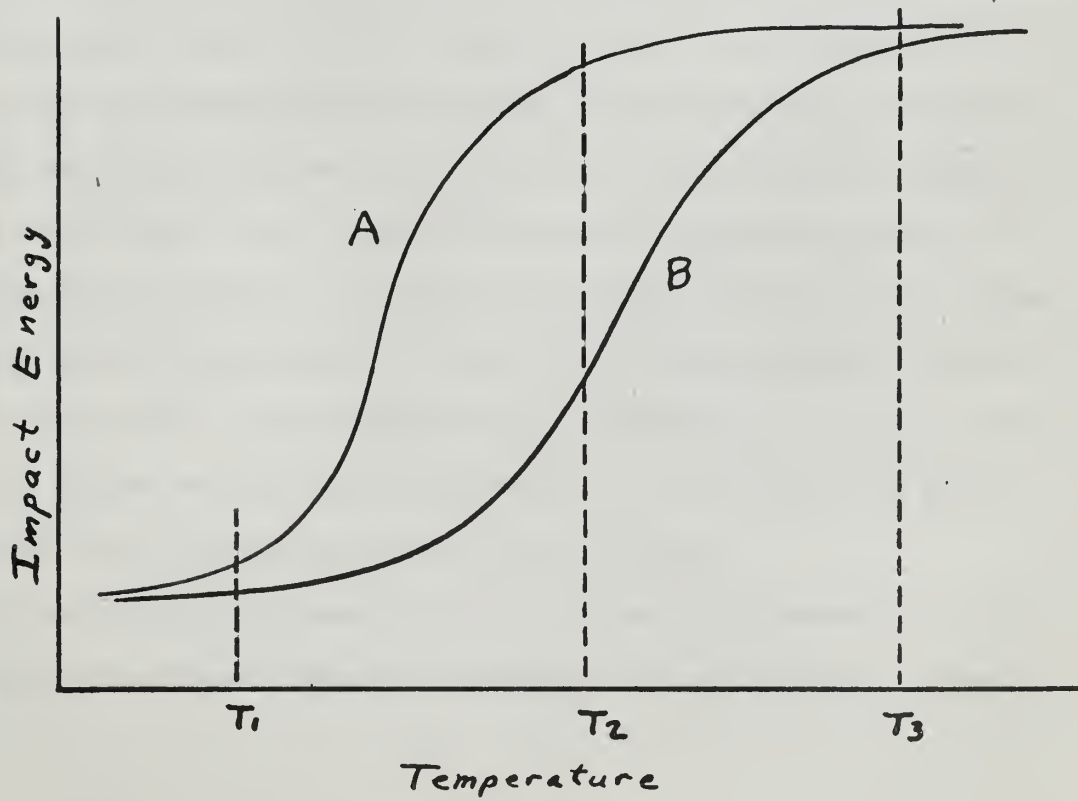


Figure 2.

during World War II when many merchant ships broke in two. To meet this serious threat to the war effort the Secretary of the Navy convened a Board of Investigation to inquire into the design and methods of construction of welded steel merchant ships. The Board traced the failures to the brittle behavior of steels and much of what is now known about the brittle characteristics of steel at reduced temperature has come as a result of the work of this Board. After the war the Board of Investigation was dissolved. The Secretary of the Treasury then established a permanent post-war group, known as the Ship Structure Committee. The aim of this committee has been to conduct a continuing research program for the improvement of the design, materials, and methods of fabrication of ship structures.

M. L. Williams⁷ has discussed the problem of ship failures quite extensively. He points out the need to reduce stress concentrations which might result from design details, welding defects, accidental damage, or metallurgical effects of arc strikes or fabricating operations. It appears that by keeping all these factors in mind during the design and through the building stages, the problem of brittle fracture in ships is fairly well in hand. In a sense the results of temper brittleness in engineering structures are reasonably well understood; i.e., the problem is known to exist and methods to avoid it are being practiced. Actually Greaves and Jones⁸ in 1925 found that the embrittlement in carbon steels could be reduced or removed by the addition of Mo. However the actual mechanism that is taking place is not well resolved.

Although brittle failures in ships received wide spread publicity, failures have not been limited exclusively to floating vessels. Many

non-ship failures have been reported⁹, probably one of the most spectacular being the molasses tank incident that occurred in January 1919 in Boston, Mass. Twelve persons were drowned in molasses or died of injuries, forty other were injured and many horses were drowned. Houses were damaged, and a portion of the Boston Elevated Railway structure was knocked over. Considerable confusion arose as to the cause of this catastrophe. The experts of the day were called in and could not produce a satisfactory explanation. In 1925, after years of testimony, the decision was handed down that the tank failed by over-stress and not by an explosion, as some of the experts had postulated.

The purpose of this thesis is to examine the phenomenon of temper brittleness to see if it is possible to correlate the embrittlement with stacking faults in the crystal.

2. Theory

Several explanations have been postulated to explain the cause of temper brittleness, some of which include a precipitation of carbide from ferrite, the presence of nitrides, and intercrystalline cracking. The precipitation of a carbide has been the most favored explanation but no evidence has been adduced to confirm this and there is little agreement among various investigators.

Faulting in Crystals

The detection and measurement of stacking faults in crystals has been discussed by many authors, notably Barrett^{10,11,12}, Warren¹³, Guentert and Warren¹⁴, Mering¹⁵, Hirsch and Otte¹⁶, Paterson¹⁷, and Wagner, Tatelman, and Otte¹⁸. Stacking faults can be thought of as mistakes in the ordered sequence of planes of atoms in a crystal. They may result from imperfect crystal growth, from plastic deformation, or from phase transformations. It has been found that faulting is quite extensive in crystals of the layer structure type, such as graphite or mica, where interatomic forces between the atoms of a layer are stronger than the forces between layers¹⁰. This layering effect is not as apparent in metals because of the non-directional nature of metallic bonds, but none the less is present as will be described.

To get a better understanding of what is meant by the "ordered sequence of planes", let us first consider the face centered cubic (FCC) structure since this is a little easier to understand than the body centered cubic (BCC) structure with which we are really concerned. The FCC structure is shown in figure 3.

In the FCC metals, the (111) planes are close packed hexagonal layers,

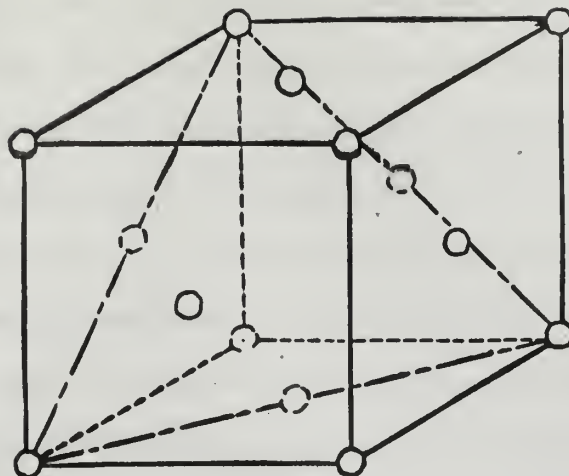


Figure 3. Face Centered Cubic Structure Showing the (111) Plane.

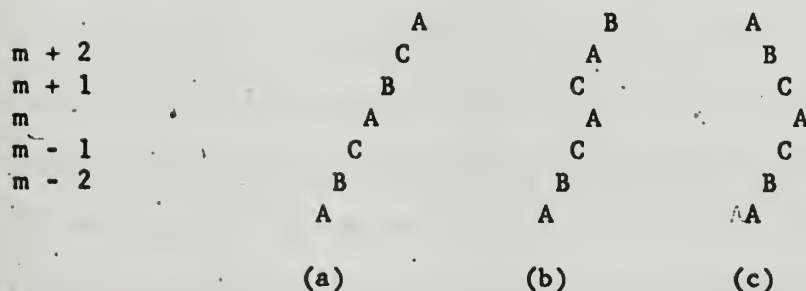


Figure 4. Faulting on the (111) planes of a FCC metal.

- (a) Normal FCC Sequence
- (b) Single deformation fault
- (c) Growth or twin fault

and the three-dimensional structure is produced by a proper stacking of these layers. This plane is indicated by the dot dash lines in figure 3. If this layer is used as a base and the atoms are considered as hard spheres, it can be seen that the atoms of each layer fit into triangular holes of the preceding layer. It should be noted here that the first ball in the second layer will have two choices of a triangular hole to occupy, and once having determined its position, the regular stacking sequence is established. If one were to look in a direction normal to the layers, three sets of atomic positions would be observed, which are usually designated ABC. The sequence ABCABC... is considered a normal FCC stacking sequence and is shown in figure 4(a).

If the m th layer in a crystal is A and the $(m + 1)$ th layer is B, slip on the (111) planes might shift everything above the m th layer as indicated in figure 4(b) so that the $(m + 1)$ th layer becomes C. It is thus said that a deformation stacking fault has been introduced between the m th and $(m + 1)$ th layers. Figure 4(c) shows a twin fault. A deformation fault thus represents a jog in an otherwise regular sequence, while a twin fault represents a reversal of the regular sequence. Either kind of faulting puts the atoms in the $(m - 1)$ th and $(m + 1)$ th layers in identical positions. The fault represents a shear in the (111) plane of $1/6 (2\bar{1}\bar{1})$ which is not a lattice vector, but which, because of the geometry of the structure, results in correct bond angles and distance between nearest neighbors. However, the fault does alter second nearest neighbor bond angles and distances.

In the BCC metals, the twinning plane is the (112) plane and is the only plane on which faulting can occur, even though the (110) plane is the most densely packed¹². The positions of the atoms are as shown in

figure 5¹⁶ and the sequence $A_1 A_2 B_1 B_2 C_1 C_2$ is called a regular stacking sequence. A sequence of six layers now defines the stacking arrangement while only three was needed for the FCC structure. Successive layers are displaced relative to each other by a vector with components $1/6$ $[1\bar{1}\bar{1}]$ and $1/2$ $[\bar{1}10]$ along the $[1\bar{1}\bar{1}]$ and $[\bar{1}\bar{1}0]$ axes respectively as can be seen in figure 5. A fault occurs when B_2 is followed by B_1 instead of being followed by C_1 . The displacement of B_1 relative to B_2 has components $-1/3$ $[1\bar{1}\bar{1}]$ and $[\bar{1}\bar{1}0]$ along the axes, and since displacements of $[\bar{1}\bar{1}0]$ cannot be distinguished inside the crystal, the fault is effectively produced by a displacement $-1/3$ $[1\bar{1}\bar{1}]$, which is also equivalent to a displacement $1/6$ $[1\bar{1}\bar{1}]$ in the $[1\bar{1}\bar{1}]$ direction. Faults are therefore produced by wrong displacements in the $[1\bar{1}\bar{1}]$ direction only.

Growth faults can occur in BCC structures in essentially the same way they did in FCC structures, giving rise to the sequence $A_1 A_2 B_1 B_2 C_1 C_2 A_1 C_2 C_1 B_2 B_1 \dots$ which produces a twin orientation. In contrast to the FCC case, these faults do not preserve nearest neighbor distances and a slight geometrical expansion of the lattice is necessary in the BCC structure although not in the FCC. This expansion is small and since the fraction of faulted crystal is also small, it is neglected in diffraction peak shape analysis.

It should be pointed out that the characteristic ductile-to-brittle transition occurs only in the BCC metals, of which steels are the most important structural example. FCC metals do not undergo this transition and are easily worked at all temperatures. The hexagonal close packed structures do have a temperature dependent ductility range but it is not

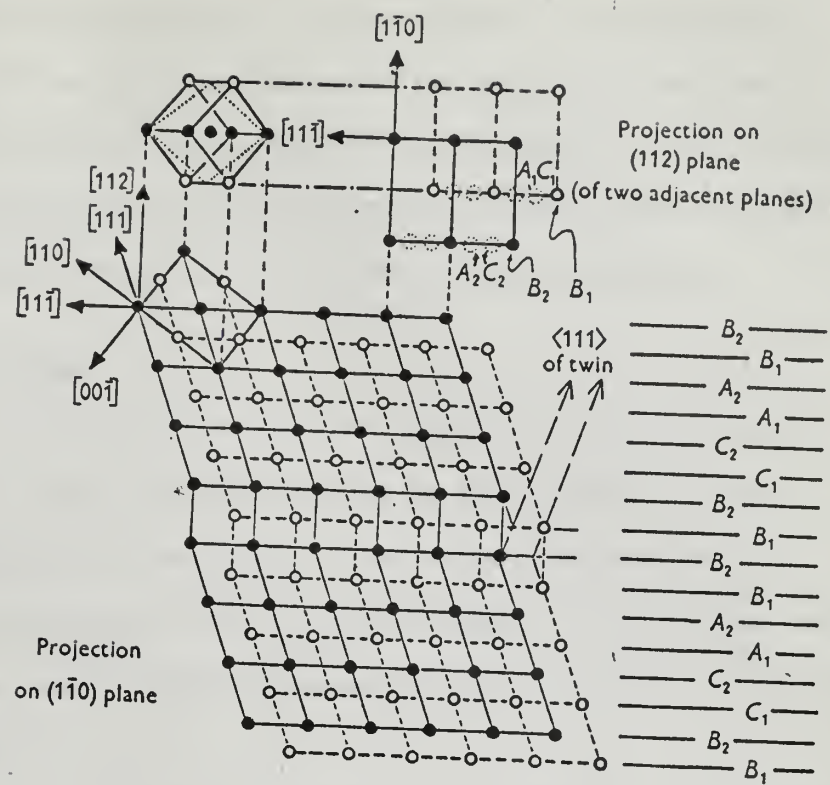


Figure 5. Projection of the BCC structure on a (112) and a (110) plane; the latter projection shows the effect of an error in the stacking sequence of the (112) planes.¹⁶

as pronounced as the BCC structure. Hahn and Jaffee¹⁹, in their study of brittle behavior of metallic and non-metallic materials, have summarized some of the factors that influence brittle behavior. These include electron bonding, crystal structure, and degree of order. The only concern in the present investigation is with the crystal structure.

Fracture and Dislocations

Ductile fracture, which occurs in most metals at elevated temperatures, usually takes place when the material is loaded above a "yield" limit and is accompanied by considerable plastic deformation. Brittle fracture occurs at temperatures that are low compared to the melting point, with little, if any, plastic deformation and fracture may occur under very low external stresses.

Plastic deformation is associated with the movement of dislocations through the lattice and when the dislocations can no longer move under an applied stress, fracture occurs.

Two kinds of dislocation motions have been distinguished²⁰; motion in the glide plane, called glide motion, and motion in which the dislocation leaves its glide plane, called climb motion. The first type of movement is that which constitutes the macroscopic phenomena of slip in crystals. It is an easy kind of motion in solids which have nondirectional bonding forces between the atoms, as for example in metals. The energy needed to bring a dislocation from one position to another in the same glide plane is small. When the dislocation climbs to a neighboring glide plane, one row of atoms has to be removed or added and this can only take place by diffusion, or else a row of interstitials or vacancies is formed.

In either case, an activation energy for the climb process must be supplied. In most metals climb occurs only at elevated temperatures, where it leads to the phenomena of polygonization²¹.

When a material is work hardened, dislocations exert stress fields and forces on each other, tending to lock them and tie them together in dislocation networks. The result is that plastic flow cannot take place until the stress is great enough to move the dislocations that have been pinned. If the normal component of this force becomes great enough to overcome the binding forces across the plane, the crystal ruptures.

Cottrell supposes that in steels an "atmosphere" of carbon atoms tends to form about a dislocation. The carbon atoms tend to go away from the pressure region and into the tension region. This process is believed to stabilize the dislocations and make it more difficult for them to move.

In the case where a dislocation is pinned and others try to move against it, or dislocations are piled up against an obstacle, the applied stress pushes the dislocations in sequence on a particular glide plane towards the lead dislocation. This lead dislocation becomes pressed hard against the obstacle and the pressure of other dislocations has the effect of magnifying the applied stress on the lead dislocation. The importance of this effect is that it enables a slip band containing many dislocations to develop a stress concentration around the obstacle sufficient to cause fracture. This is essentially what is supposed to take place during brittle fracture, dislocations "pile up" and cause fracture at a low applied stress.

Read has shown how faults can act as barriers to dislocations²². Let us consider a fault that extends completely through a crystal, and let

slip take place on a plane that intersects this fault. If the slip vector is not parallel to the fault, the intersecting slip cuts the fault into two halves, which are displaced parallel to the slip vector. Each of these halves has a boundary within the crystal and these boundaries are defined as partial dislocations. The slip that cuts the fault has to supply the energy to create the partial dislocations. Therefore a fault is a barrier to slip on an intersecting plane.

The difference between faults arresting a dislocation and faults at which dislocations are formed is their orientation relative to the slip plane. Only faults in a favorable position can produce stress concentrations in the slip direction and thus dislocations. The stress field of the arrested dislocations opposes the external force field and this effect is greater the higher the density of dislocations. This actually leads back to the explanation of work hardening, a phenomena we have already encountered.

Partial Dislocations and Faulting.

In some instances a dislocation can lower its energy by splitting into two partial dislocations whose Burgers vectors are not lattice translation vectors. For a complete dislocation to dissociate into partials it is necessary that the two partials have an elastic energy of repulsion sufficiently intense to overcome surface tension effects of misfit surface between these partials. There will be an equilibrium separation of the partials where the repulsive force, which decreases with distance, is just equal to the constant surface tension of this misfit area. A dislocation having a $1/2 [110]$ slip vector in a FCC crystal could lower its energy by dissociating into two partials (Shockley partials) having

slip vectors $1/6 [2\bar{1}\bar{1}]$ and $1/6 [\bar{1}21]$ respectively, and connected by a stacking fault, which can be visualized as follows²³. Consider the crystal to be made up by stacking spheres in close packing. When one close-packed layer has been laid down, the second layer can be added in two ways as has been pointed out and the normal sequence of layers was given before as being ABCABC... Now if slip of $1/6 [2\bar{1}\bar{1}]$ occurs, corresponding to moving a layer into a neighboring set of triangular holes, then above the fault $A \rightarrow B$, $B \rightarrow C$, and $C \rightarrow A$, so that the sequences of planes become ABCABCBCABC... The sequence BCBC is of the hexagonal close-packed type and thus defines a stacking fault in the FCC crystals.

These Shockley partial dislocations can move in their slip planes by slipping motions, however, they cannot move out of their slip planes either by cross slip in another plane or by diffusion because a partial dislocation is necessarily tied to a misfit surface. The misfit surface is defined by the vector displacement of the adjoining atomic planes. A stacking fault is defined by a $1/6 [112]$ type displacement, which corresponds to a low energy misfit on a $(1\bar{1}1)$ plane but to a high energy misfit on any other plane; hence the partials can move only on the plane of their connecting fault.

Frank²⁴ has discussed another type of partial dislocation which has been called a sessile dislocation, because it cannot move at all by slipping. For example, if a complete $1/2 (110)$ dislocation combined with a $1/6 [\bar{1}\bar{1}2]$ Shockley partial, the result would be a $1/3 [111]$ partial attached to the stacking fault of the original Shockley partial. This configuration could be made with a sphere model by making a cut part way through the crystal on a (111) plane and inserting a layer of atoms to produce an ABCBCABC... stacking fault. The slip vector $1/3 [111]$ of

this partial dislocation on the boundary of the extra plane is at right angles to the plane of the stacking fault; hence, since the dislocation cannot move out of the plane of its fault, it cannot move by slipping but only by diffusion and this, as has been mentioned, requires higher energy.

Thus faulting, by introducing "partial" and "sessile" dislocations, can restrict the amount of plastic deformation, not only because these dislocations, introduced by faults are themselves immobile, but because they also serve to "pin" other dislocations.

Measurement of Faulting by Fourier Analysis of X-ray Diffraction Peak Shapes

A Fourier series is a type of infinite trigonometric series by which any kind of periodic function may be expressed. The one essential property of a crystal is that its atoms are arranged in space in a periodic fashion. This means that the density of electrons is also a periodic function of position in the crystal, rising to a maximum at the point where an atom is located and dropping to a low value in the region between atoms. To regard a crystal in this manner, as a positional variation of electron density rather than as an arrangement of atoms, is particularly appropriate where diffraction is involved, in that X-rays are scattered by electrons and not by atoms as such. Since the electron density is a periodic function of position, a crystal may be described analytically by means of a Fourier series. This method of description is very useful in structure determination because the coefficients of the various terms in the series are related to the structure factor or F values of the various X-ray reflections.

Since the X-ray diffraction pattern of a crystal is the Fourier transform of the electron density in the crystal, Warren and Averbach²⁵ demonstrated that a Fourier analysis of X-ray diffraction peaks can be employed

to measure the atomic displacements responsible for the peak broadening observed from cold worked crystals. Their pioneer work has been extended to study distortions produced under a variety of conditions.

In order to apply a Fourier analysis, peak shapes are measured using monochromatized X-rays and a Geiger counter. These shapes are then corrected for instrumental broadening by the method of Stokes²⁶. Each peak from an annealed specimen is represented by a Fourier series; the corresponding peak from a cold worked specimen is also represented by a Fourier series, and from the coefficients of the two series a third set of coefficients is computed for a series that represents the shape of the corrected line.

The manner in which the Warren-Mering analysis of diffraction peak shapes is extended to include faulting in the crystal can be seen from the following. Consider a general distortion in which the position of an atom in a unit cell $m_1 m_2 m_3$ is given by the vector R . In terms of the unit cell vectors a_1 , a_2 , and a_3 ,

$$R m_1 m_2 m_3 = m_1 a_1 + m_2 a_2 + m_3 a_3 + \delta m_1 m_2 m_3$$

The term $\delta m = X m a_1 + Y m a_2 + Z m a_3$, is different, in general, for each cell $m = m_1 m_2 m_3$, and represents the elastic distortion remaining in a plastically deformed crystal. These displacements are small enough so that coherent scattering still takes place over small volumes of the crystal.

Let the direction of the primary and diffracted X-ray beams be represented by the unit vectors S_0 and S , so that their difference gives

$$S - S_0 = \lambda (h_1 b_1 + h_2 b_2 + h_3 b_3)$$

where b_1 , b_2 , and b_3 are the vectors of the reciprocal lattice and h_1 , h_2 , and h_3 are continuous variables. The intensity from the crystal is then related to the displacement at pairs of cells, at $Rm_1m_2m_3$ and $Rm_1'm_2'm_3'$, by the relation

$$I(h_1h_2h_3) = F^2 \sum_{m_1} \sum_{m_2} \sum_{m_3} \sum_{m'_1} \sum_{m'_2} \sum_{m'_3} e^{(2\pi i/\lambda)(S - S_0)} (R_m - R_{m'})$$

This distribution of intensity in reciprocal space is then integrated throughout reciprocal space so as to give the power in the corrected plot of intensity distribution vs. 2θ in a diffraction peak. For convenience crystal axes a_1 , a_2 , a_3 are chosen so that each reflection is of the type (001). The result of integration is expressed as a Fourier series

$$P_{2\theta} = K \sum_{n=-\infty}^{\infty} A_n \cos 2\pi n h_3$$

where $n = m_3 - m_3'$, $h_3 = 1/\lambda (2a_3 \sin \theta)$, and the Fourier coefficients are $A_n = \langle \cos 2\pi 1 \cdot Z n \rangle_{av}$ where the displacement is $Z n = Zm_3 - Zm_3'$, the component of δ_m in the Z direction, and the averaging is carried out over all pairs of cells separated n cell lengths apart in a given column of cells parallel to a_3 , and over all such columns in the crystal. The general procedure is then to plot the A_n values from the experimental data vs. n . The shape of this curve is different for different causes of line broadening and it is thus possible to determine the contributing causes. For example, microstresses give a curve that has zero slope at $n = 0$, while crystallite size gives a finite slope at $n = 0$, the slope being determined by the effective average size.

Paterson¹⁷ extended the Warren-Mering technique to include faulting as an additional cause of line broadening in cold worked FCC metals by calculating the probability of the additional terms which should be

included in the displacement δ if the probability of a fault occurring on any given layer of the crystal is α . He derived the following equation relating the Fourier coefficients to the probability of faulting produced by random slip on a single set of FCC (111) planes:

$$A_n = [\sqrt{1-3\alpha(1-\alpha)}]^{1/2}$$

The analysis relates line broadening to the indices of a scattering plane and if twin faults are present predicts an asymmetrical broadening of some of the peaks. The probability of twining, β , can under some circumstances be determined from the Fourier coefficients of the asymmetrical peaks. Further, a peak displacement is predicted which can also be related to faulting probabilities.

Guentert and Warren¹⁴ extended the analysis to include faulting in cold worked BCC structures. As was shown earlier, stacking faults in the BCC structure are produced by wrong components of displacement in the $[11\bar{1}]$ direction. In the unfaulted crystal successive (112) planes are displaced relative to each other by a vector with a component $1/6 [11\bar{1}]$ in the $[11\bar{1}]$ direction. Since each layer has equivalent atomic positions at 0 and $1/2 [11\bar{1}]$, a sequence of only three layers (with position at 0, $1/6 [11\bar{1}]$, and $1/3 [11\bar{1}]$) is needed to describe the pattern of displacements along the $[11\bar{1}]$ direction, as can be seen in figure 5. Thus, if only the positions of the layers along the $[11\bar{1}]$ axis is considered, the sequence can be described simply as ABCABC... Hence the calculations for the probability of finding a fault at any of the three positions along the $[11\bar{1}]$ axis reduces to that relevant to the FCC case, and those results can be adapted to the BCC structure. The assumption is made that the two kinds of faults, stacking and twin faults,

occur independently and at random on the (112) planes. One problem in the analysis of the cold worked BCC structures occurs since all lines are made up of components that are shifted in opposite ways by deformation faults on the (112) planes, and as Guentert and Warren¹⁴ have shown, there is no net displacement of a line due to this type of fault. Thus the small magnitude of line shifts expected from twin faults may be obscured making reliable measurements difficult. In the FCC case involving cold work, a peak shift was predicted. Wagner et al¹⁸ suggest that perhaps there are peak shifts in BCC structures.

3. Experimental Work

The specimen used in this study of temper brittleness was a standard 3140 steel which was known to be susceptible to embrittlement²⁷. In view of the difficulty in obtaining reproducible results and in interpreting the results of continuous cooling experiments, which were attempted, temper brittleness was produced in this investigation entirely by isothermal treatments following methods outlined by Jaffe, Carr, and Buffum.²⁷ Pellini and Queneau²⁸, in a study of the effects of micro-structure on temper brittleness, found that tempered martensite is somewhat more susceptible to embrittlement than is tempered pearlite. Thus only two basic structures, or specimens, were observed, ductile tempered martensite and embrittled tempered martensite.

A group of Charpy impact specimens were austenitized in a salt bath at 925°C (1540°F) for one hour and then water quenched to produce martensite. The Rockwell "C" hardness was 53 ± 2 . The specimens were then tempered in another salt bath for one hour at 654°C (1210°F) and then water quenched. The Rockwell hardness was then $Rc 22 \pm 1$. Half of the specimens were kept as tempered martensite while the other half were given an embrittling treatment consisting of 48 hours in a salt bath at 500°C (932°F) after which they were water quenched. The Rockwell "C" hardness of this group was about 17. Salt baths were used exclusively in this treatment to ensure a close control over the temperature and also to prevent surface oxidation and decarburization. An oil quench was tried initially but it was found that the oil and particles from the salt bath reacted quite vigorously on the surface of the specimens causing considerable pitting. Thus water was used as the quenching medium in view of the possibility of quench cracks.

The specimens were examined for cracks using Zyglo ZL1B dye penetrant and ZP4 dry powder developer. Many specimens were observed to have cracks and these were held aside for the X-ray investigation. More samples were prepared for an impact test and this time they were quenched in warm water (115°F). The crack frequency dropped from about 75% to about 25% using this technique.

The ductile and embrittled specimens were broken at various temperatures using a Tinius Olsen 264 ft-lb impact tester which was built to ASTM specifications E23. A "warming curve" was established to determine the various temperatures subsequently used in breaking the specimens. This was accomplished by inserting a calibrated copper constantan thermocouple into a specimen so that it was located under the notch of the specimen. The specimen and thermocouple were immersed in a dewer which contained dry ice and acetone at a temperature of -80°C for 20 minutes. They were then placed in the breaking position on the impact tester. The temperature was observed as a function of time while the specimen was warming up to room temperature. Several runs were conducted and a plot of temperature vs. time was made. This plot was used to determine the various temperatures at which the specimens were broken.

The results of breaking the specimens proved that the treatment outlined above for embrittlement definitely gave two distinct samples. Curves of impact energy vs. temperature were then plotted and found to be similar to the curves obtained by Jaffe, Carr, and Buffum²⁷ for matensite. The differences were probably due to the fact that their results were based on more test data. This phase of the experimental work was merely to demonstrate a real difference in the two specimens, not to reproduce the transition temperature curves.

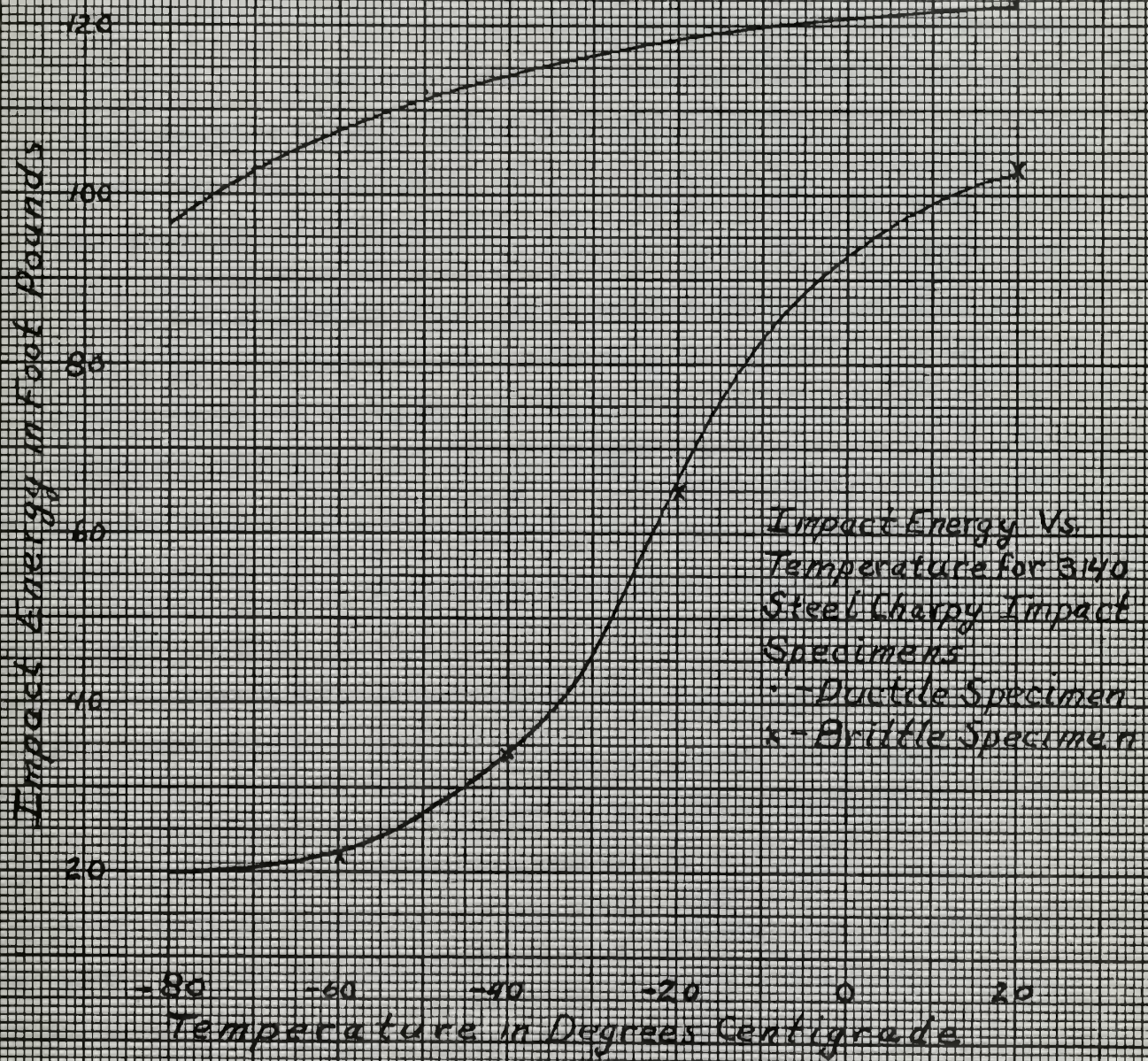


Figure 6. Impact Energy Vs. Temperature

The specimens held aside for X-ray diffraction were electropolished using a Buehler Ltd. 1721-2 electropolisher with a 1721-1AB power source and a standard electrolyte recommended for low carbon steels.

A Phillips Norelco X-ray unit with a high precision goniometer was used for the X-ray diffraction with a Xenon filled proportional counter. A single channel, model 510, pulse height analyzer, manufactured by Atomic Instrument Co. of Cambridge, Mass., was used in lieu of a single crystal monochromator or filter. Various peak shapes were traced out on the Brown potentiometer for both the ductile and embrittled specimens using Mo, Co, and Cr radiation. Frequently the statistics with the xenon counter were rather poor, especially when it had a quantum efficiency of about 30%. Some curves were traced out by a point by point method using a fixed time of 64 seconds. It was found that this was not completely satisfactory due to poor statistics and the best curves were obtained by running the one particular curve desired several times, both in the forward and backward direction, then superimposing these on one another and tracing out the curve shape.

The (112) β peak was observed at room temperature, -47°C (-52°F), and 90°C (194°F) using Cr radiation. These results will be discussed in a later section. The low temperature was obtained by immersing part of the specimen in a bath of dry ice and acetone. A copper constantan thermocouple was clamped to the side of the specimen near the irradiated surface to check the temperature. Chips of dry ice were frequently added to maintain the temperature at a constant value. It was found that a 250 watt heat lamp placed close to the specimen would heat it to 90°C . This temperature could be held constant by adjusting the distance of the bulb to the specimen.

It was the authors intent to analyze the curves resulting from the X-ray differraction by means of a Fourier analysis. Due to insufficient time, the particular program being adapted to the CDC 1604 computer could not be straightened out and hence the results are being offered on a qualitative basis only.

4. Results

The Charpy impact tests discussed earlier served to demonstrate the fact that the two specimens were different, i.e., one was ductile and the other embrittled. A plot of the impact energy vs. temperature is shown in figure 6. These results are in agreement with previous investigators²⁷.

From the curves produced by X-ray diffraction three significant effects were observed. These were (1) a slightly better resolution of the alpha doublet by the embrittled specimen, (2) a relative peak displacement between similar lines from the ductile and brittle specimens, and (3) a noticeable asymmetry in some of the peak shapes from both specimens.

The better resolution of the alpha doublet is in agreement with work done by Jacquet, Buckle, and Weill²⁹. Woodfine² has pointed out that this slightly better resolution is probably due to the fact that internal stresses present after quenching a specimen from 500°C will be lower than those in a specimen quenched from 654°C. Figures 7 and 8 showing the (112) alpha peaks with Cu radiation demonstrate this difference in resolution.

The relative peak displacement between the ductile and brittle specimens was apparent in almost all patterns recorded and became more pronounced at higher angles. The effect, moreover, always occurred in the same direction, i.e., the diffraction peaks of the brittle specimen came at higher 2θ values than the ductile specimen, never lower values. This effect can be seen in figures 7 and 8. A relative displacement, always in the same direction, would indicate some sort of expansion in the

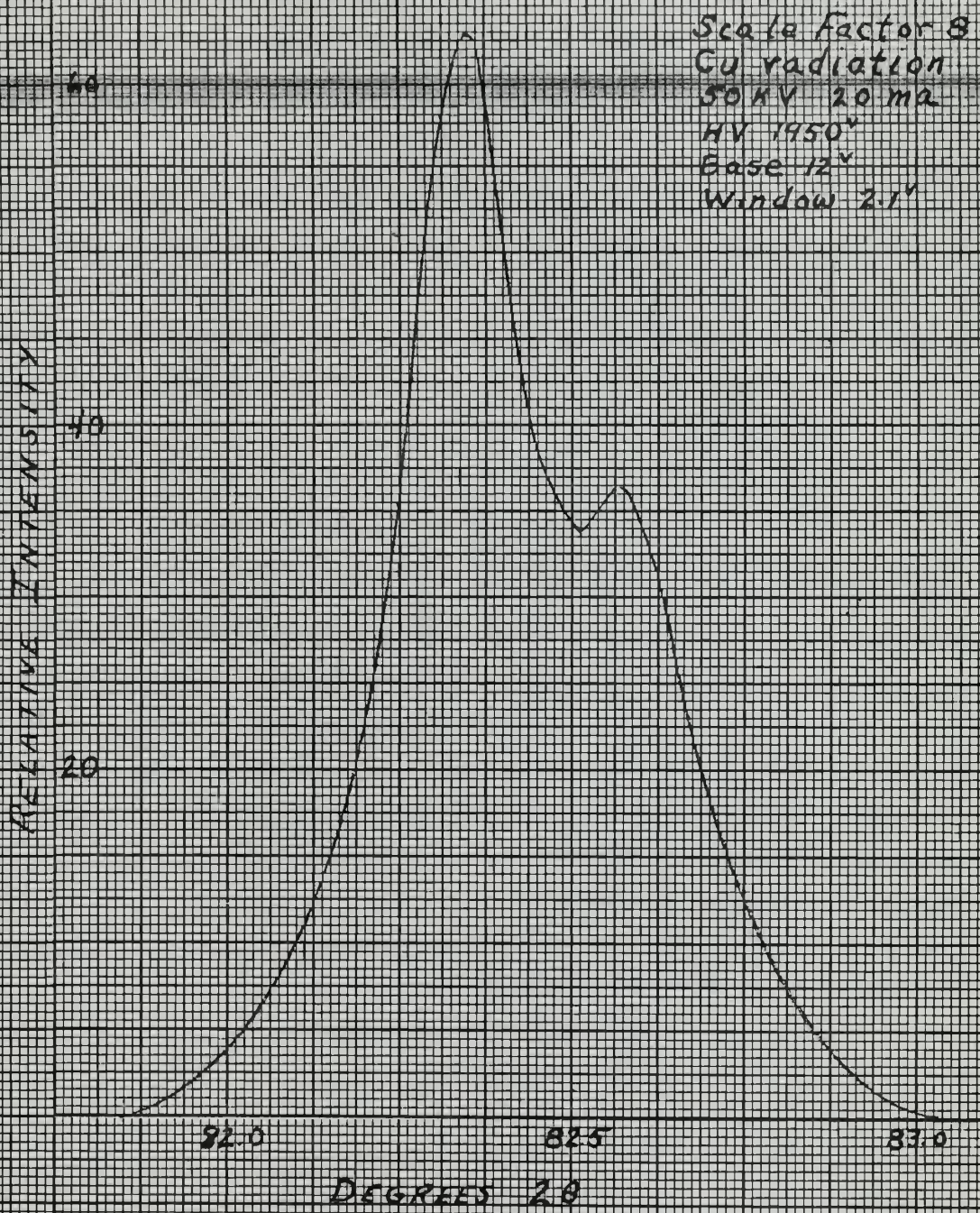


Figure 7 (112) $\bar{\alpha}$ Peak Ductile Specimen

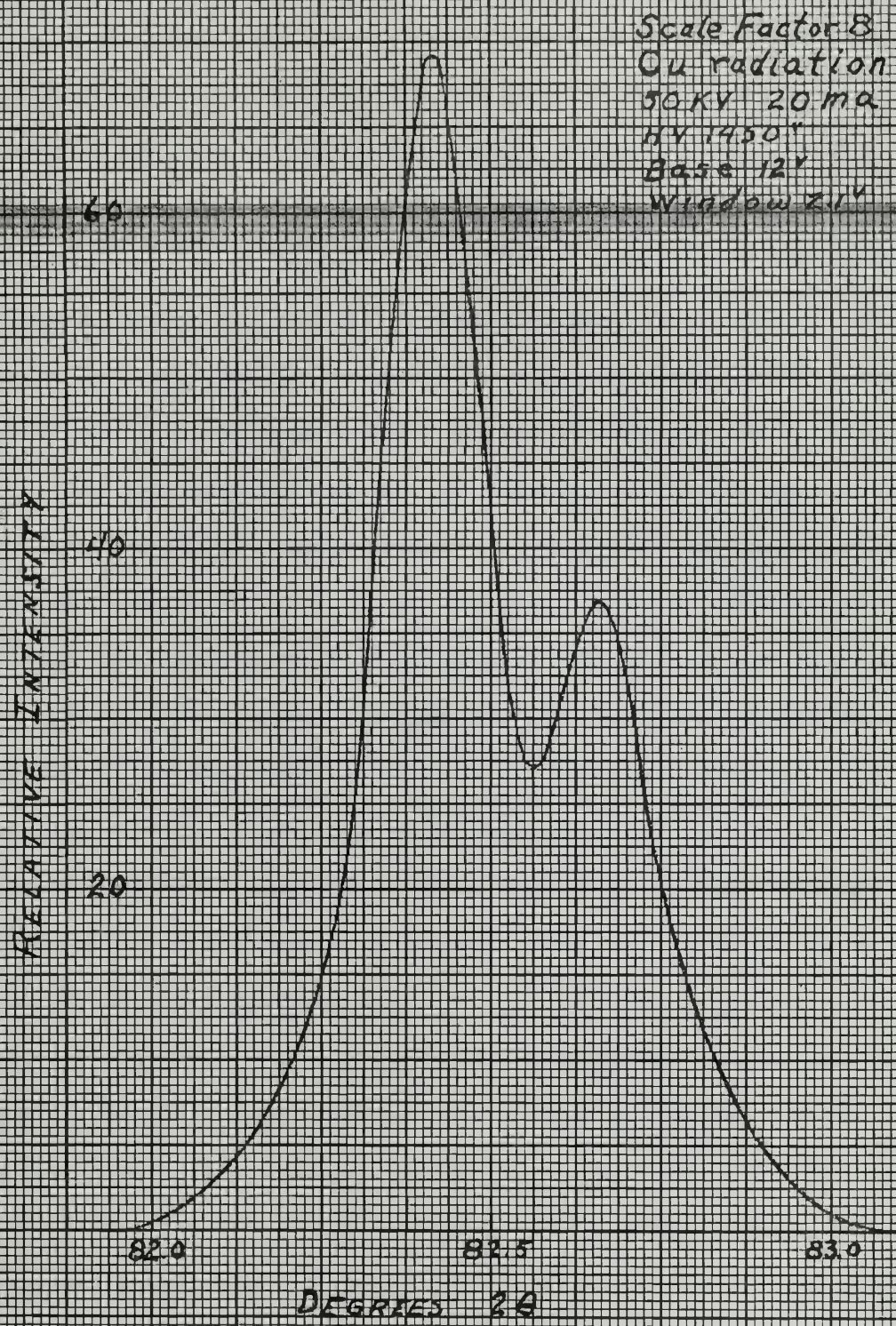


Figure 8 511210¹ Peak Brinell Specimen

lattice or a difference in the lattice parameter. Values of the lattice parameter were computed for both the ductile and brittle specimens, based on the many different diffraction peaks obtained. These computed a - values were then plotted vs. $\cos^2 \theta / \sin \theta$. A straight line should result, which extrapolated to zero, would give a true value of the lattice parameter. In spite of the scatter, two distinct straight lines could be drawn through the points giving a value of 2.8674 \AA for the ductile specimen and 2.8659 \AA for the embrittled one. Since this portion of the experimental work was not intended to give a precise value of the lattice parameters, the absolute values are not of real significance, however the difference in their values, 0.0015 \AA , is significant. Maloof³⁰ has reported a similar difference of 0.0006 \AA between his ductile and embrittled specimens. This difference in lattice parameter could be due to the expansion in the lattice caused by faulting, to a precipitation effect, or possibly a combination of the two effects. Recall that the expansion in a BCC lattice, mentioned earlier, is small, and was neglected in the Fourier analysis. This might indicate that the expansion should not be neglected.

The alpha doublets were resolved following the method outlined by Rachinger³¹, and the initial asymmetry persisted in the peak shapes. The peaks which showed this asymmetry in both alpha and beta components were the (110), (220), and the (211), the (200), (310), (222), (312), and (330) appeared symmetrical. Typical (110) curves are included in figures 9 and 10. Figure 9 shows the asymmetry in the (110) beta peak and figure 10 shows the asymmetry in the (110) alpha peak after the Rachinger correction has been applied.

REFRACTIVE INDEX

60

40

20

17.5

18.0

18.5

DEGREES 29

Scale Factor 2
Mo radiation
50 KV 20 ma
HV 1325^x
Base 10⁴
Window 2.1^y

Figure 9. (110) Peak Brittle Specimen

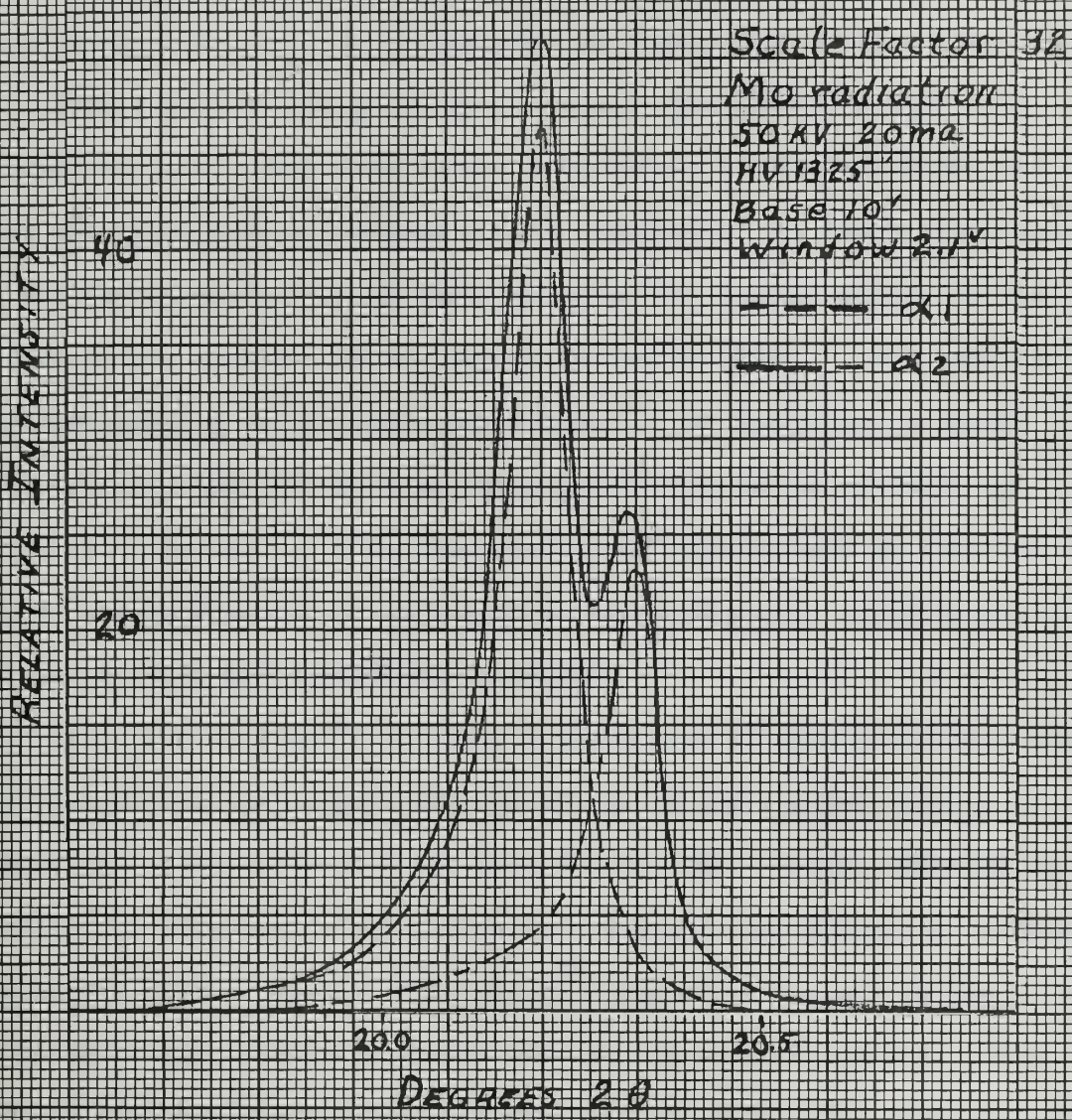


Figure 10: (Mo) α Peak Ductile Specimen

Results of Other Workers Using the Electron Microscope

Maloof³⁰ in 1952 and Woodfine³² in 1953, studied ductile and embrittled specimens using the electron microscope. Both looked for a difference in the precipitate between the two specimens and were unable to detect any noticeable difference. Thomas³³ describes various techniques that have aided greatly in the interpretation of results of electron diffraction. He recommends that specimen tilting be used in all crystal work to bring out good contrast and also to avoid false interpretations. Many details are revealed by tilting which are not otherwise apparent, such as twinned areas. Another of the newer techniques is the "moiré pattern". In these patterns the lattice planes of the structure are resolved in the magnified "moiré image." The smallest resolved spacing so far reported is 5.8 \AA ³⁴, or just about a whole order of magnitude better than the electron microscope of about ten years ago. Because of these aforementioned improvements in electron microscopes and techniques, it is possible that differences could be detected between ductile and embrittled specimens.

Kelly and Nutting³⁵, in their observations of martensite with the electron microscope, report the appearance of small precipitates, presumably ϵ - carbide, across the twin bands. This causes hardening by locking the only remaining deformation system in an internally twinned martensite plate. Hatwell and Votava³⁶ have observed twin dislocations in an austenitic stainless steel with the electron microscope. They suggest that the elastic field of dislocations piled upon coherent twin boundaries could induce the movement of partial dislocations during a precipitation heat treatment. These partial dislocations distributed along the coherent twin boundaries constitute sites for the preferential

nucleation of a precipitate.

A similar effect has been suggested by Willis³⁷ in a discussion on FCC alloys. He has considered diffraction effects to be expected from FCC alloys showing segregation and predicts an asymmetry due to segregation. He also suggests that faults, which have been shown to exist in FCC structures, present sites where the segregates are trapped, and that trapping at these faults would modify the asymmetrical diffraction peaks. Barrett³⁸ has commented on segregation of impurities at grain boundaries and points out a need for further investigation of the role of these impurities in the fracture process.

In the BCC structure extensive faulting can occur even in the absence of cold work. It seems probable that segregation would also develop at these faults and likewise modify the symmetry of the diffraction peaks. However, no analysis has yet been suggested which distinguishes between the asymmetry due to segregation and that due to faulting in the BCC structures.

In an attempt to learn more about the transition curve, the (112) beta peak was observed, using Cr radiation, at -47°C, room temperature, and 90°C. Using the room temperature peak position as a standard, the expected peak shift due to the temperature effect was computed. Within experimental error, this was the result actually observed. The asymmetry of the peaks did appear to change and this may be seen in figures 11 - 16 which show the ductile and brittle peak shapes at each of the three temperatures. A comparison of the peak shapes of the ductile specimen at 90°C and -47°C reveals very little difference, while this same comparison of the brittle peak shapes shows a significant difference.

This observation can be correlated with the change in impact energy, shown in figure 6. It can be seen that the difference in impact energy for the ductile specimens over this range is quite small compared to the difference in the brittle specimens over the same range.

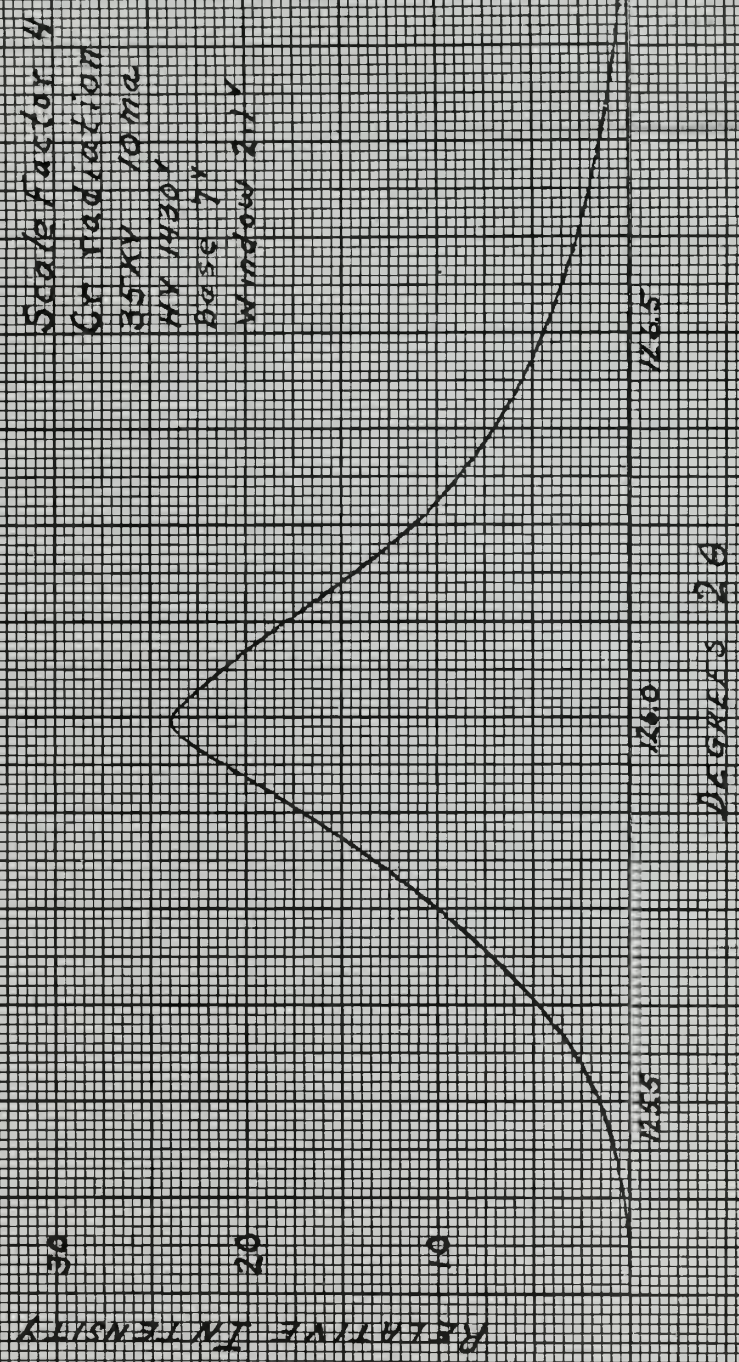


Figure 11. (1/2) Peak Doublet Specimen Temperature = 40°C

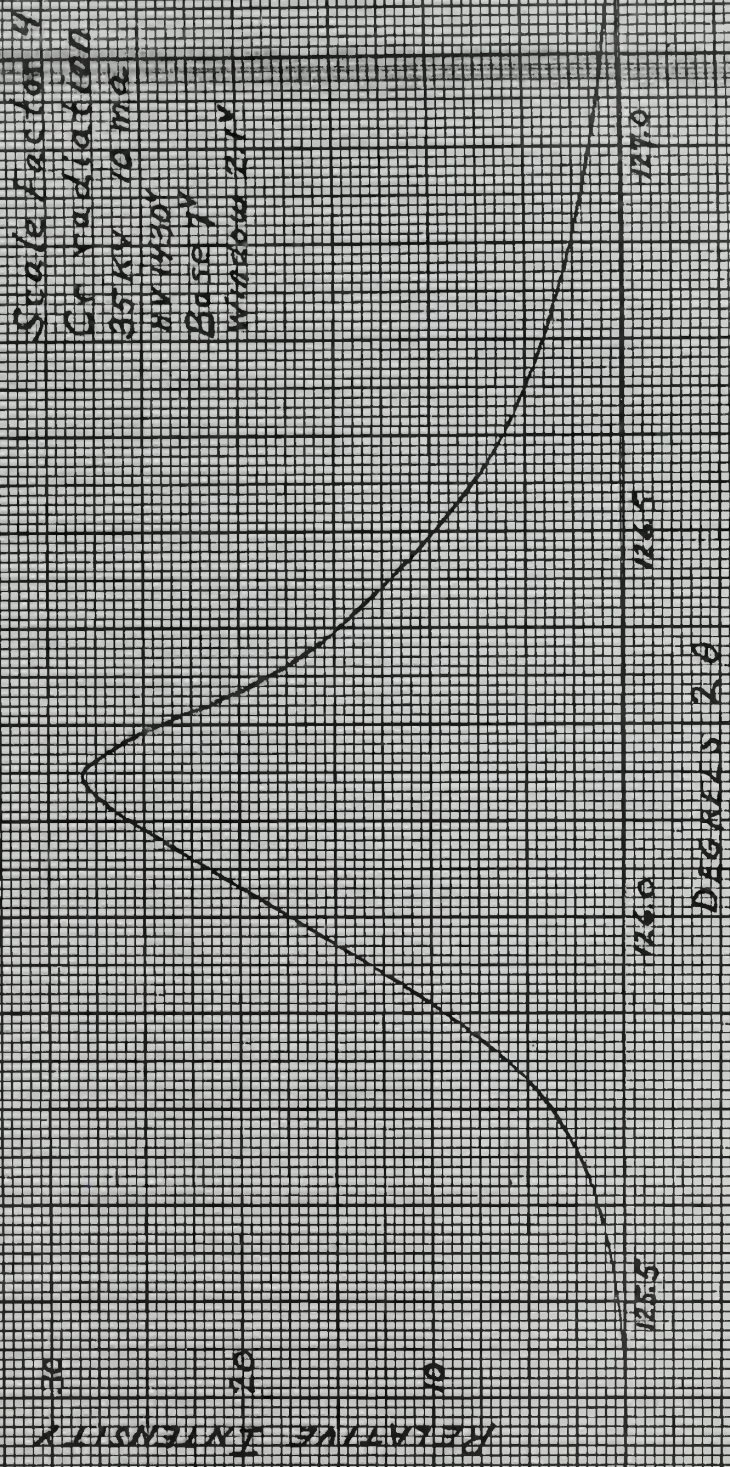


Figure 12. Peak Brittle Specimen Temperature 44°C

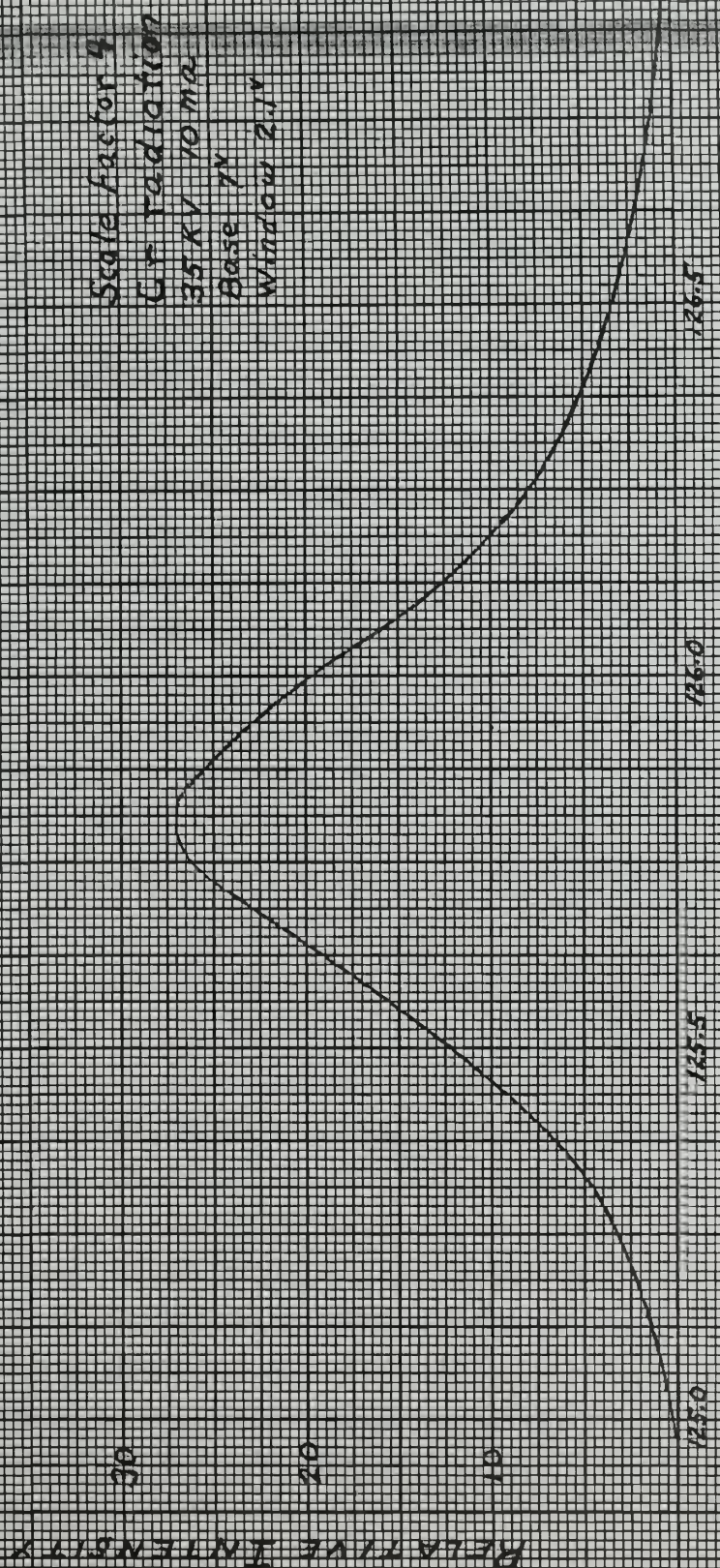


Figure 13. $\alpha/2/\beta$ peak. Ductile Specimen Room Temperature

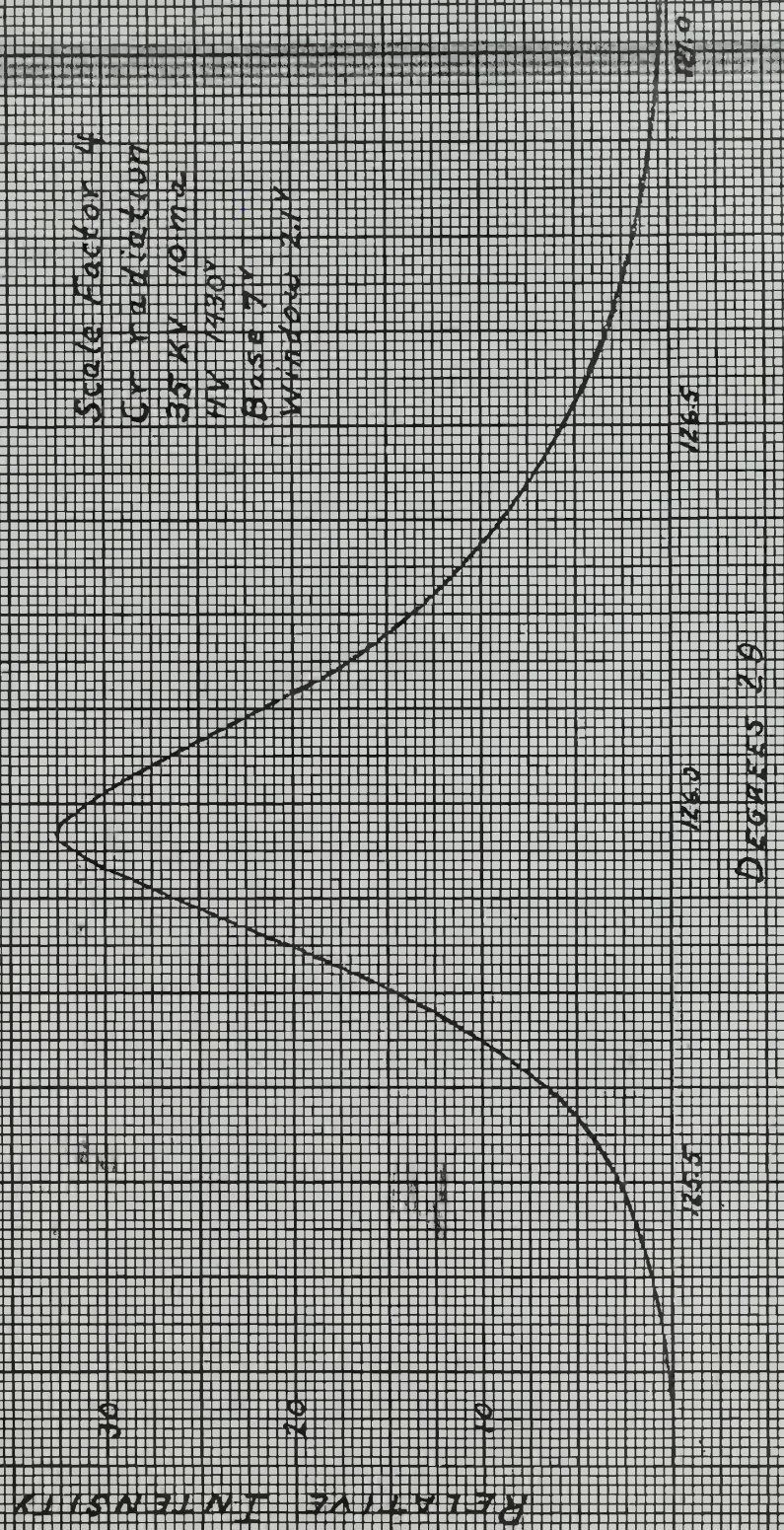


Figure 14. (112) β Peak. Brittle Specimen. Room Temperature

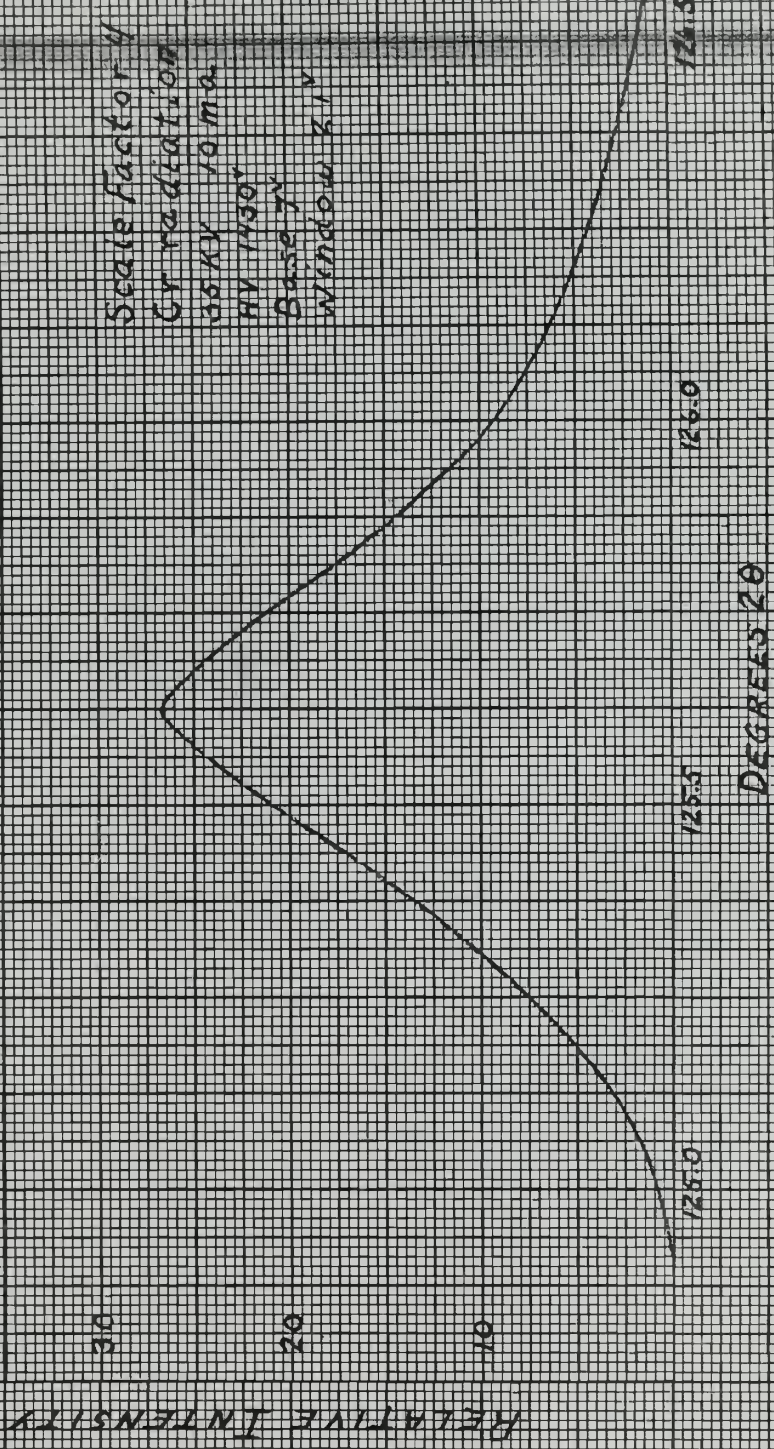


Figure 15. (112) β peak Ductile Specimen Temperature 90°C

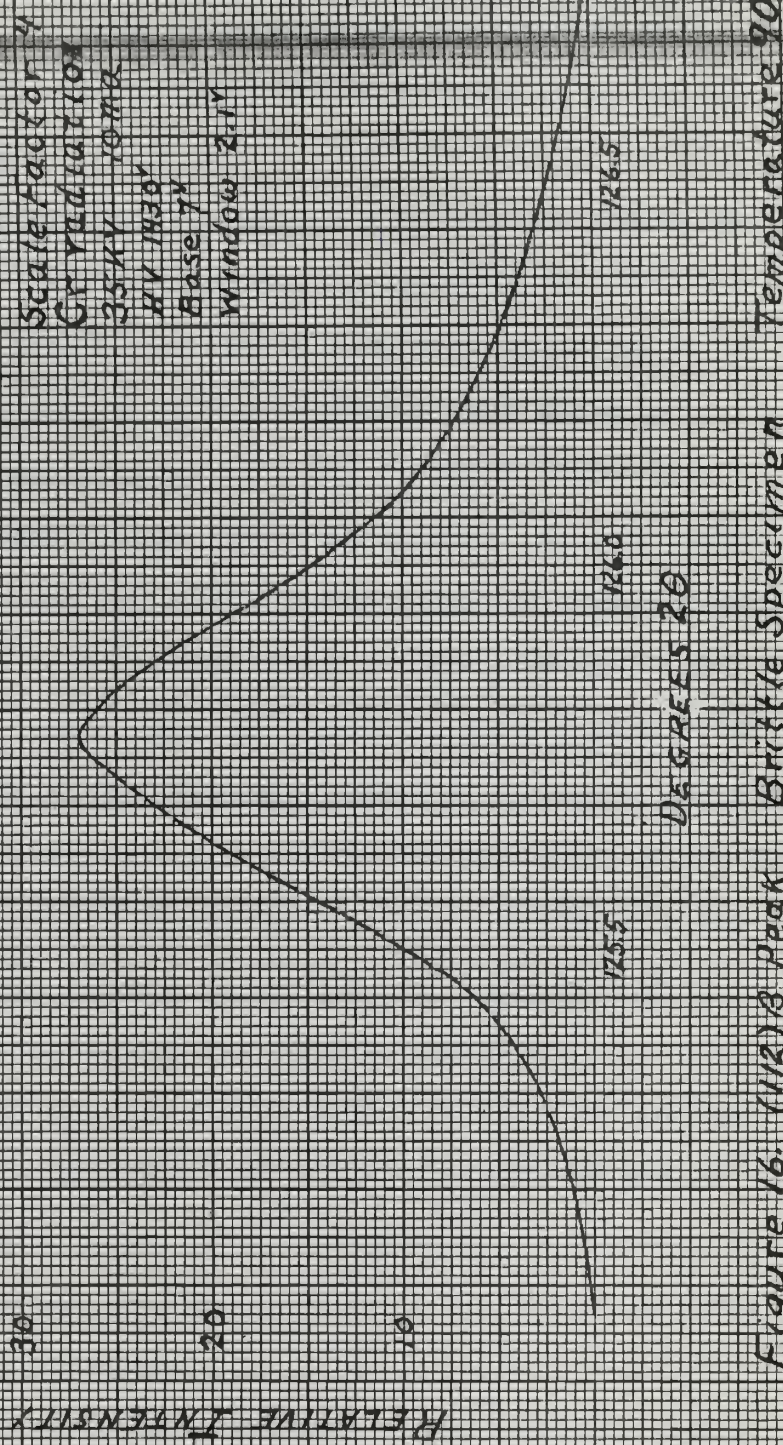


Figure 16. 11/210 Peak. Brittle Specimen. Temperature 90°C

5. Conclusions

The results mentioned previously, particularly the asymmetry of some of the diffraction peak shapes, indicate that faulting occurs in both specimens. Without a Fourier analysis of the peak shapes, only quantitative comments can be made in comparing the faulting in the ductile and embrittled specimens.

The experimental observations do indicate a correlation between embrittlement and faulting. The difference in asymmetry between the (112) beta peak shapes for the brittle specimen at room temperature and -47°C, figures 12 and 14, can be related to the transition curve shown in figure 6. There is a change of about 70 ft-lbs in impact energy and at the same time, a noticeable change in the asymmetry of the peak shapes. The ductile specimen does not show such a marked change in asymmetry which could be explained by the fact that the change in impact energy is only 10 ft-lbs over this same range. Thus the transition curve suggests that as the temperature decreases, the faulting probability increases, and the dislocations are pinned. This is a more reasonable explanation of the loss of ductility and the transition temperature than the formation of a carbide since much less energy is required to form the faults than for a precipitate to go in or out of solution. As the temperature is lowered, faults tend to move closer together and any existing faults and precipitates will prevent the movement of dislocations. Now, under an applied stress, brittle failure will occur. This is suggested as a possible explanation of the temperature dependent portion of the transition range in the ductile-to-brittle transition.

The increase in the transition temperature of the embrittled specimen is possibly due to segregation, or a precipitate, which in addition

to the faulting, serves to pin dislocations as mentioned earlier, and thus leads to a brittle type of failure at a higher temperature.

These suggestions are made on the basis of the experimental observations. A Fourier analysis could help confirm or reject these ideas.

For future work, it is suggested that the X-ray diffraction patterns be taken at a temperature corresponding to T_2 in figure 2. This temperature corresponds to the largest difference in impact energy between the two specimens and the diffraction peak shapes should show, correspondingly, the greatest amount of difference.

The electron microscope could show differences in any precipitate, and if one is not available, possibly a small angle scattering technique could be used to detect precipitants or segregates.

BIBLIOGRAPHY

1. Holloman, J. H., *Transactions of the A.S.M.*, 36, 473, 1946.
2. Woodfine, B. C., *J. Iron Steel Inst.*, 173, 229, 1953.
3. Polushkin, E. P., *Defects and Failures of Metals*, Elsevier Publishing Company, New York, 1956.
4. Queneau, B. R., *The Embrittlement of Metals*, A.S.M., Cleveland, Ohio, 1956.
5. Metals Handbook, A.S.M., Cleveland, Ohio, 1961, p. 38,39.
6. Jolivet, H., and G. Vidal, *Rev. Met.*, 41, 387, 1944.
7. Williams, M. L., in *Symposium on Effect of Temperature on the Brittle Behavior of Metals with Particular Reference to Low Temperatures*, A.S.T.M., Philadelphia, 1954, p 11.
8. Greaves, R. H., and J. A. Jones, *J. Iron Steel Inst.*, 111, No. 1, 231, 1925.
9. Shank, M. E., in *Symposium on Effects of Temperature on the Behavior of Metals with Particular Reference to Low Temperatures*, A.S.T.M., Philadelphia, Pa., 1954, p 45.
10. Barrett, C. S., in *Imperfections in Nearly Perfect Crystals*, John Wiley & Sons, Inc., New York, 1952, p 97.
11. Barrett, C. S., *Structure of Metals*, Second Edition, McGraw-Hill Book Company, Inc., New York, 1952, p 380.
12. Barrett, C. S., in *Cold Working of Metals*, A.S.M., Cleveland, Ohio, 1949, p 65.
13. Warren, B. E. *Progress in Metal Physics*, Vol 8, Pergamon Press, New York, 1959, p 147.
14. Guentert, O. J., and B. E. Warren, *J. Appl. Phys.*, 29, 40, 1958.
15. Mering, J., *Acta Cryst.*, 2, 371, 1949.
16. Hirsch, P. B., and H. M. Otte, *Acta Cryst.*, 10, 447, 1957.
17. Paterson, M. S., *J. Appl. Phys.*, 23, 805, 1952.
18. Wagner, C. N. J., A.S. Tatelman, and H. M. Otte, *Office of Naval Research Contract S.A.R. - Nonr 609(43)* March 1962.

Bibliography (Continued)

19. Hahn, G. T., and R. I. Jaffee, "A Comparison of the Brittle Behavior of Metallic and Nonmetallic Materials", DMIC Memorandum 107, May 16, 1961.
20. Cottrell, A. H., *Dislocations and Plastic Flow in Crystals*, The University Press, Oxford, 1953.
21. Van Bueren, H. G., *Imperfections in Crystals*, North-Holland Publishing Company, Amsterdam, 1960.
22. Read, W. T., *Dislocations in Crystals*, McGraw-Hill Book Company, Inc., New York, 1953.
23. Read, W. T., and W. Shockley, in *Imperfections in Nearly Perfect Crystals*, John Wiley & Sons, Inc., New York, 1952.
24. Frank, F. C., *Proc. Phys. Soc. (London)*, 62, 202, 1949.
25. Warren, B. E., and B. L. Averbach, *J. Appl. Phys.*, 21, 595, 1950.
26. Stokes, A. R., *Proc. Phys. Soc.*, 61, 382, 1948.
27. Jaffee, L. D., F. L. Carr, and D. C. Buffum, *Journal of Metals*, 5, 1147, 1953; Buffum, D. C., and L. D. Jaffee, *ibid* p 1373.
28. Pellini, W. S. and B. R. Queneau, *Trans. A.S.M.*, 39, 139, 1947.
29. Jacquet, P. A., H. Buckle, and A. R. Weill, *Compt. Rend.*, 231, 411, 1951.
30. Maloof, S. R., *Trans. A. S. M.*, 44, 264, 1952.
31. Rachinger, W. A., *Journal Scien. Inst.*, 25, 254, 1948.
32. Woodfine, B. C., *J. Iron Steel Inst.*, 173, 240, 1953.
33. Thomas, G., *Transmission Electron Microscopy of Metals*, John Wiley & Sons, Inc., New York, 1962.
34. Bassett, G. A., J. W. Menter, and D. W. Pashley, *Proc. Roy. Soc.*, 246, 345, 1958.
35. Kelly, P. M., and J. Nutting, *J. Iron Steel Inst.*, 197, 199, 1961.
36. Hatwell, H., and E. Votava, *Acta Met.*, 9, 945, 1961.
37. Willis, B. T. M., *Acta Cryst.*, 12, 683, 1959.
38. Barrett, C. S., in *Fracture*, Edited by Averbach et al, published jointly by The Technology Press of MIT and John Wiley & Sons, Inc., New York, 1959.

